Retention of Inhibitory Potency of an ACE Inhibitor Conjugated with Rh(III) and Pd(II) (Iminophosphorano)phosphines. Synthesis and X-ray Structural Investigations

Raghoottama S. Pandurangi,*,†,‡ Kattesh V. Katti,§ Loreen Stillwell,|| and Charles L. Barnes‡

Contribution from the Department of Internal Medicine, Department of Chemistry, and Department of Radiology and Missouri University Research Reactor, University of Missouri, Columbia, Missouri 65211, and Monsanto, Chesterfield Pkw. St. Louis, Missouri 64321

Received January 21, 1998

Abstract: Succinimido, amido, and ester functionalized tetrafluoroaryl azides selectively oxidize bisdiphenylphosphinomethane at one of the P(III) centers giving (iminophosphorano)phosphines **6**, **7**, and **8** respectively in high yields. Succinimido functionalized perfluoroaryl azido (iminophosphorano)phosphine is attached to angiotensin converting enzyme (ACE) inhibitor, lisinopril at one end, leaving the other end for chelation to Rh(III) and Pd(II) precursors including radioactive analogues establishing the hetero-bifunctionality for potential in vivo tracking of the radiotracer. The measurement of inhibitory potency of lisinopril−metal conjugates (Rh and Pd), modified through the primary amine reveals an increase in inhibitory potency, although small, retaining the target potential of native lisinopril toward specific biological sites. However, direct complexation utilizing the carboxylic groups of lisinopril with a Cu precursor resulted in the reduction of inhibitory potency from nM to μM levels rendering it less useful for applications as an ACE inhibitor. Single-crystal X-ray structural investigation of the Rh(III) perfluoroaryl (iminophosphorano)phosphine complex **12** shows a distorted mer octahedral configuration with two ligands per metal center and only one of the phosphiniminato nitrogen atom coordinating to the metal. Pd(II) complex **18** reveals that the metal is bound to the iminato nitrogen atom and the P(III) center via cis disposition to form a five-membered ring. X-ray data for **12**: triclinic, P-1, $a = 11.570$ (6) Å $b = 13.668$ Å(7) $c = 20.709$ (10) Å, $\alpha = 86.068$ (10), $\beta = 83.774$ (10), $\gamma = 83.503$ (10) $V = 3229.6$ (3) Å^3, $Z = 2$, $R = 0.028$, $R_w = 0.050$. X-ray data for **18**: triclinic, P-1, $a = 11.457$ (3) Å, $b = 12.223$ (3) Å, $c = 13.219$ (4) Å, $\alpha = 89.98$ (20), $\beta = 73.710$ (20), $\gamma = 69.980$ (20), $V = 1665.7$ (8) Å^3, $Z = 2$, $R = 0.024$, $R_w = 0.031$.

Introduction

Angiotensin converting enzyme (ACE, EC 3.4.15.1) is a zinc metalloprotease enzyme which catalyzes the hydrolysis of carboxy-terminal dipeptides from oligopeptide substrates.[1−3] ACE is an important component of the renin−angiotensin system (RAS) associated with the biological conversion of angiotensin I (AI) to angiotensin II (AII), a vasoconstrictor shown to be partly responsible for hypertension.[4] Recent studies[5] have revealed the anatomic concordance of high-density binding of ACE with fibrous tissue formation in the failing human heart. An impressive array of ACE inhibitors (e.g., lisinopril, captopril, etc.) and their ^{125}I analogues are shown to inhibit the overexpression of ACE in vivo and to suppress fibrosis in animal models.[6] This observation indicates that ACE inhibitors have a high target potential toward specific biological sites rich in ACE. Functionalization of ACE inhibitors by bifunctional chelating agents (BFCAs) carrying radiometals (e.g., ^{99m}Tc or ^{105}Rh) adds diagnostic potential to the already established target potential of ACE inhibitors and may open a new possibility of tracking them to specific biological sites in vivo. Lisinopril, a lysine analogue of enalapril ([s]-Na-[1-carboxy-3-phenylpropyl]-lys-prolin), is a clinically proven drug for the treatment of hypertension[7−9] and hence, attachment of a clinically useful transition metal radiotracer permits non-invasive monitoring of ACE-related activity in human beings since ^{125}I-lisinopril is limited to only animal studies.

* To whom the correspondence to be addressed.
† Department of Internal Medicine, University of Missouri.
‡ Department of Chemistry, University of Missouri.
§ Department of Radiology and Missouri, University Research Reactor.
|| Monsanto.

(1) (a) Johnson, C. I. *Drugs* **1990**, *39*, 21. (b) Campbell, D. J. *J. Clin. Invest*. **1987**, *79*, 1. (c) Ehlers, M. R. W; Riordan J. F. *Biochemistry* **1990**, *28*, 5311. (d) Ehlers, M. R. W.; Riordan J. F. In *Hypertension: Pathophysiology, Diagnosis and Management*; Laragh, J. H., Brenner, B. M., Eds.; Raven Press: New York, 1989. (e) Campbell, D. J. *J. Clin. Invest.* **1987**, *79*, 1. (f) Erdos, E. G. *J. Lab. Invest.* **1987**, *56*, 345 (g) Ondetti, M. A.; Cushman D. W. *Annu. Rev. Biochem*. **1982**, *51*, 283. (h) Bunning, P.; Holmquist; Riordan, J. F. *Biochemistry* **1983**, *22*, 103.

(2) (g) Soffer, R. L. *Annu. Rev. Biochem*. **1976**, *45*, 73. (h) Soffer, R. L. In *Biochemical Regulation of Blood Pressure*; Soffer, R. L., Ed.; Wiley: New York, 1981; pp 123−164.

(3) Ondetti, M. A.; Cushman, D. W. *J. Med. Chem*. **1981**, *24*, 355.

(4) Elisiva, Y. E.; Orekhovich, V. N.; Pavlikhina, L. V.; Alecsenco, L. P. *Clin. Chim. Acta* **1971**, *31*, 413.

(5) Weber, K. T. Inflammation and Healing in the heart . In *Wound Healing in Cardiovascular Disease*; Weber, K. T., Ed.; Futura Publishing Co. Inc: Armonk, NY, 1995; pp 1−21.

(6) (a) Sun, Y.; Cleutjens, J. P. M.; Diaz-Arias, A. A.; Weber K. T. *Cardiovasc. Res.* **1994**, *28*, 1423. (b) Sun, Y.; Ratajska, A.; Zhou, G.; Weber K. T. *J. Lab. Clin. Med.* **1993**, *122*, 395.(c) Sun, Y.; Ratajska, A.; Zhou, G.; Weber K. T. *J. Lab. Clin. Med.* **1995**, *126*, 95. (d) Sun, Y.; Weber K. T. *J. Mol. Cell Cardiol.* **1996**, *28*, 851. (e) Sun, Y.; Weber K. T. *J. Lab. Clin. Med.* **1996**, *127*, 94. (f) Weber, K. T.; Sun Y.; Katwa, L. C. and Cleutjens, J. P. M. *Basic Res. Cardiol*. **1997**, *92*, 75.

10.1021/ja9802403 CCC: $15.00
Published on Web 10/22/1998

Cavel et al.[10] have established the combination of phosphine and iminophosphorane, produced by a selective oxidation of one of the diphosphines, as versatile chelating agents to several transition metals including Rh(I). The recent studies[11] on the extension of the coordination chemistry of iminophosphoranes to the diagnostically useful transition metal ^{99m}Tc and their stability in aqueous medium indicates that these conjugates are potential in vivo tracking agents, provided they are conjugated to a pharmacophore of interest. Since ^{99m}Tc has a short half-life[12] (6.5 h), we have used Rh- and Pd-based BFCAs for the present studies. ^{105}Rh has a low abundance of γ-rays ($E\gamma$ = 306 keV, 5%, 319 keV, 19%) which would allow in vivo tracking of drugs[13] at specific biological sites. However, the major requirements for radiometalated ACE inhibitors to be diagnostic agents include (a) the establishment of the coordination chemistry of Rh(III) including the geometrical configuration of the chelate ring with respect to the binding sites of lisinopril and (b) the confirmation of the retention of the inhibitory potency of ACE inhibitors, functionalized by relatively bulky and electron-rich metalated chelating agents. In our earlier studies, we have shown that functionalization of lisinopril at the primary and secondary amine groups by tetrafluoroaryl azides has improved their binding potency, assessed by autoradiography studies,[14] competitive radioligand binding assays,[14] molecular dynamics calculations,[15] and IC_{50} measurements using amydolytic assays.[15] Since attachment of perfluoroaryl azides to lisinopril shows promising inhibitory potency, further functionalization of azides by phosphines provides a needed lisinopril−BFCA conjugate ready to incorporate transition metals and analogous radiometals. Selective oxidation of one of the phosphines of diphosphines provides asymmetrically substituted (iminophosphorano)phosphine combination which is expected to improve the stability of the complex through bidentate coordination to metal.[16,17]

Our interest here is to identify the best site on lisinopril for further functionalization and to test the effect of metalated chelating frameworks at different sites of lisinopril (primary amine group, secondary amine group, carboxylic groups, etc.) on the inhibitory potency of lisinopril conjugates in the post modification. Although Rh(III) complexes with phosphines are known[16,17] and Rh(I)−(iminophosphorano)phosphine complexes are quite common,[18] surprisingly, Rh(III)−(iminophosphorano)-phosphines are uncommon. Since ^{105}Rh is available in a virtually "no carrier added" version as $Rh(III)Cl_3 \cdot xH_2O$, the ultimate success of the ACE-inhibitor avid radiopharmaceutical as an in vivo tracking agent depends on the precise structural determination of the nonradioactive Rh(III) complex in solid form and its conformation in solution. Hence, as a part of the ongoing research on BFCAs[19] and bifunctional photolabile chelating agents (BFPCAs),[20] we wish to elucidate the X-ray structural investigations on representative Rh(III) and Pd(II) perfluoroaryl functionalized (iminophosphorano)phosphines, supplemented by multinuclear and 2D NMR of functionalized lisinopril derivatives. We also would like to establish the retention of the inhibitory potency at nM level for primary amine functionalized Rh(III) and Pd(II) conjugates, in contrast to functionalization at carboxylic groups with a Cu complex which resulted in the significant loss of activity. These findings constitute a first report on the biological activity of lisinopril, tailored by metalated chelating agents.

Experimental Section

All synthetic procedures were conducted in a dry nitrogen atmosphere using standard Schlenk tube techniques and prepurified solvents. Reactions involving the synthesis of azides were carried out in a subdued light by wrapping the flasks with aluminum foil. Nuclear magnetic resonance spectra were recorded in $CDCl_3$ on a Bruker WH-300 spectrometer, and chemical shifts are reported in ppm downfield from $SiMe_4$ for ^{1}H NMR. The ^{31}P NMR chemical shifts are reported with respect to 85% H_3PO_4 as an external standard, and positive shifts lie downfield from the standard. ^{19}F NMR chemical shifts are reported

(7) (a) Bohacek, R.; Lombaert, S. D. McMartin, C.; Priestle, J.; Grutter, M. *J. Am. Chem. Soc.* **1996**, *118*, 8231. (b) Wyvratt, M. J.; Patchette, A. A. *Med. Res. Rev.* **1985**, *5*, 483. (c) Opie, L. H. *Angiotensin Converting Enzyme Inhibitors*; Wiley-Liss: New York, 1992. (d) Squire, I. B.; Lees, K. R. *Rev. Contemp. Pharmacother.* **1994**, *4*, 45. (e) Lawton, G.; Pacioreck, P. M.; Waterfall, J. F. The design and biological profile of ACE inhibitors. In *Advances in Drug Research*; Jovanovich, H. B., Ed.; Academic Press: New York, 1992; Vol. 23, pp 161−220.

(8) (a) Edwards, C. R. W.; Padfield, P. L. *Lancet* **1985**, 30. (b) Johnston, C. I. *Med. J. Aust.* **1988**, *148*, 488. (c) Patchett, A. A. Enalapril and Lisinopril. In *Chronicles of Drug Discovery*; Lednicer, D., Ed.; ACS Professional Reference Book, American Chemical Society: Washington, DC, 1993; Vol. 3, pp 125−162. (d) Goa, K. L.; Balfour, J. A.; Zuanetti, G. *Drugs* **1996**, *52*, 564.

(9) (a) Mendelsohn, F. A. O. *Clin. Exp. Pharmacol. Physiol.* **1984**, *11*, 431. (b) Reid, J. L. *J. Cardiovasc. Pharmacol.* **1993**, *22 (suppl)*, s 41.

(10) (a) Reed, R. W.; Santarsiero, B.; Cavell, R. G. *Inorg. Chem.* **1996**, *35*, 4292. (b) Li, J.; McDonald, R.; Cavell R. G. *Organometallics* **1996**, *15*, 1033. (c) Balakrishna, M. S.; Klein, R.; Uhlenbrock, S.; Pinkerton, A.; Cavell R. G. *Inorg. Chem.* **1993**, *32*, 5676. (d) Li, J.; Pinkerton, A. A.; Finnen, D. C.; Kumar, M.; Martin, A.; Weisemann, F.; Cavel, R. G. *Inorg. Chem.* **1996**, *35*, 5684.

(11) (a) Katti, K. V. Singh, P. R. Katti, K. K.; Barnes, C. L.; Kopica, K.; Ketring, A. R.; Volkert, W. A. *Phosphorus, Sulfur Silicon Relat. Elem.* **1993**, 55. (b) Jurisson S.; Eble, E.; Berning, D.; Barnes, C. L.; Katti, K. V. Phosphine Complexes of Technetium (VII). In *Chemistry and Nuclear Medicine*; Nicolini, M., Bandole, G.. Mazzi, U., Eds.; SGE: Padova, 1995; pp 201−203. (c) Katti, K. V.; Singh, P. R.; Katti, K. K. Kopica, K.; Volkert, W. A.; Ketring, A. R. *J. Labelled Compd. Radiopharm.* **1993**, 22, 407.

(12) Volkert, W. A.; Jurisson, S. Technetium-99m chelates as radiopharmaceuticals. In *Technetium and Rhenium their chemistry and it's applications; Topics in Current Chemistry*; Ed. by Yoshihara. K., Omori, T., Eds.; Springer Verlag: Berlin, Heidelberg, 1996; Chapter 4, pp 123−148. (b) Volkert, W. A. Ligand systems useful in designing high specific activity ^{99m}Tc or ^{186}Re, ^{188}Re radiopharmaceuticals. In *Technetium and Rhenium in Chemistry and nuclear Medicine*, 4th ed.; Nicolini, M., Mazzi, U., Eds.; Cortina International: Verona, Italy, 1995; pp 239−242. (c) Jurisson, S.; Berning, D.; Jia, W.; Ma, D. *Chem. Rev.* **1993**, *93*, 1137. (e) Meares, C. F. *Nucl. Med. Biol.* **1986**, *13*, 311. (e) Schwochau, K. *Angew. Chem., Int. Ed. Engl.* **1994**, *33*, 2258.

(13) Ehrhardt, G.J; Ketring, A. R.; Volkert, W. A. A production of isotopes at nuclear reactors. In *Synthesis and Applications of Isotopically Labeled Compounds*; Buncel, E., Kabalka, G. W., Eds.; Elsevier Science: The Netherlands, 1991; pp 159−164. (b) Goswami, N.; Alberto, R.; Barnes, C. L.; Jurisson, S. *Inorg. Chem.* **1996**, *35*, 7546.

(14) Pandurangi, R. S.; Kuntz, R. R.; Sun, Y.; Weber K. T. *Bioorg. Chem.* **1997**, *57*, 75.

(15) Pandurangi, R. S.; Rao, S. N.; Stillwell, L**;** Barnes, C. L.; Kuntz R. R. *J. Am. Chem. Soc.*, submitted.

(16) (a) Jardine, F. H.; Sheridan, P. S. In *Comprehensive Coordination Chemistry*; Eds. Wilkinson, G., Gillard, R. D., McCleverty, J. A., Eds.; Pergamon: Oxford, 1987; Vol. 4, Chapter 48.

(17) Mayer, H. A.; Kaska, W. C. *Chem. Rev.* **1994**, *94*, 1239.

(18) (a) Bader, A.; Lindner, E. *Cord. Chem. Rev.* **1991**, *108*, 27. (b) Katti, K. V.; Cavell, R. G. *Comm. Inorg. Chem.* **1990**, *10*, 53. (c) Katti, K. V.; Cavell, R. G. *Organometallics* **1988**, *7*, 2236. (d) Katti, K.V; Cavell, R. G. *Inorg. Chem.* **1989**, *28*, 413. (e) Katti, K.V.; Cavell, R. G. *Inorg. Chem.* **1989**, *28*, 3033. (f) Katti, K. V.; Cavell, R. G. *Organometallics* **1989**, *8*, 2147. (g) Katti, K. V.; Batchelor, R. J.; Einstein, F. W. B.; Cavell, R. G. *Inorg.Chem.* **1989**, *29*, 808. (h) Liu, C. Y.; Chen, D. Y.; Cheng, M. C.; Peng, S. M.; Liu, S. T. *Organometallics* **1995**, *14*, 1983. (i) Weight A.; Bischoff, S. *Phosphorus, Sulfur Silicon Relat. Elem.* **1995**, *102*, 91. (j) Katti, K. V.; Santarseiro, B. D.; Pinkerton, A. A.; Cavell R. G. *Inorg. Chem.* **1993**, *32*, 5919. (k) Law, D. J.; Bigam, G.; Cavel R. G. *Can. J. Chem. Rev. Can. De Chimie*. **1995**, *73*, 635.

(19) (a) Pandurangi, R. S.; Karra, S. R.; Kuntz, R. R.; Volkert, W. A. *Photochem. Photobiol.* **1997**, *65*, 101. (b) Pandurangi, R. S.; Kuntz, R. R.; Volkert, W. A.; Barnes, C. L.; Katti, K. V. *J. Chem. Soc., Dalton Trans.*, **1995**, 565. (c) Pandurangi, R. S.; Karra, S. R.; Kuntz, R. R.; Volkert, W. A. *Bioconjugate Chem.* **1995**, *6*, 630. (d) Pandurangi, R. S.; Kuntz, R. R.; Volkert, W. A. *Appl. Radiat. Isot.* **1995**, *46*, 233. (e) Pandurangi, R. S.; Karra, S. R.; Katti, K. V.; Volkert, W. A.; Kuntz, R. R. *J. Org. Chem.* **1997**, *62*, 2587. (f) Pandurangi, R. S.; Karra, S. R.; Kuntz, R. R.; Volkert, W. A. *Photochem. Photobiol.* **1996**, *64*, 100. (g) Pandurangi, R. S.; Katti, K. V.; Volkert, W. A.; Kuntz, R. R. *Inorganic Chemistry* **1996**, *35*, 3716.

Table 1. Summary of the Crystallographic Data for Rh Complex **12** and Pd Complex **18**

formula	$C_{34}H_{27}N_3OF_4P_2Cl_2Pd$	$C_{66}H_{50}N_2O_4F_8P_4Cl_3Rh{\cdot}CH_3CN$
MW	808.85	1461.32
crystal size (mm)	0.15 0.15 × 0.35	0.30 × 0.35 × 0.35
crystal system	triclinic	triclinic
space group	*P*-1	*P*-1
a (Å)	11.457(3)	11.5702(6)
b (Å)	12.223(3)	13.6685(7)
c (Å)	13.219(4)	20.7090(10)
α (deg)	87.980(20)	86.0680(10)
β (deg)	73.710(20)	83.7740(10)
γ (deg)	69.980(20)	83.5030(10)
U (Å^3)	1665.7(8)	3229.6(3)
F(000)	810.85	1483.5
Z	2	2
D_{calc} (g/cm^3)	1.613	1.503
$2\theta_{max}$ (deg)	45.9	54.0
μ (cm^{-1})	8.5	5.5
hkl range	−11 to 12, 0 to 13, −14 to 14	−14, 14, 0, 17, −26, 26
total data	4911	19282
unique data	4636	13299
R^a	0.024	0.028
R^b	0.031	0.050

[a] $R = \sum(|F_o| - |F_c|)/\sum|F_o|$. [b] $R' = [\sum w(|F_o| - |F_c|)^2/\sum|F_o|^2)^+$, $w^{-1} = [\sigma|F_o| + 0.0005(F^o)^2]$.

with respect to $CFCl_3$ as an external standard. Elemental analysis for the new compounds were done by Oneida Research Services, Inc., New York. Syntheses of functionalized perfluoroaryl azides (**1**−**5**) were accomplished by the methods reported earlier.[10,19] In general, organic azides are potentially explosive, and caution must be taken while preparing them.[10,17] Metallic precursors, $RhCl_3xH_2O$ and $PdCl_2(PhCN)_2$, were obtained from Aldrich. Lisinopril was a gift from Merck and was used as such without further purification.

ACE Binding Assays. Estimation of the inhibitory potency of all lisinopril derivatives was measured using amydolyic assays.[1i] About 10 μL of 0.25 μg/mL ACE (from rabbit lung) in 30 mL of buffer (50 mM HEPES containing 300 mM NaCl at pH 7.5) was mixed with various concentrations of lisinopril derivatives (10^{-12} M -10^{-6} M) and the mixture was incubated at room temperature for 10 min. The cleaving reaction was initiated with the addition of 40 μL of substrate (1.25 mM *N*-(3-[2-furyl}acryloyl)-Phe-Gly-Gly) and monitored continuously for 8 min at 340 nm using a Molecular Devices ThermoMAX plate reader. Cleavage of the substrate by the enzyme results in a product which has an absorbance at 340 nm. Binding of new lisinopril derivatives to ACE changes the cleaving potential of ACE which is reflected in the reduction of absorbance at 340 nm. The relative integration of the areas under the curve is used for computing the relative IC_{50} values of new lisinopril derivatives.

X-ray Data Collection and Processing. The crystal data and the details of data collection for crystals of **12** and **18** are listed in Table 1. X-ray data were collected on an Enraf-Nonius CAD-4 diffractometer[20,21] with Mo Kα radiation and a graphite monochromator at 22 (1) °C. The cell dimensions were obtained from a least-squares fit to setting angles of 25 reflections with 2θ in the range 20.0−30.0°. The crystal exhibited no significant decay under X-ray irradiation.

The structures were solved by direct methods and were subsequently refined by full matrix least-squares method which minimizes $\Sigma w/(|F_0| - |F_c|)^2$ where $w^{-1} = [\sigma(\text{counting}) + (0.008(F_0)^2)/4F_0]$. Atomic scattering factors including anomalous scattering contributions were from ref 21(a−g). All hydrogen atoms in both of the structures were located in difference Fourier maps and refined with fixed isotropic thermal parameters. Listing of full experimental details, coordinates, temperature factors, and anisotropic temperature factors are deposited as Supporting Information.

Synthesis of Perfluoro Functionalized Phosphinimines 6−10. A solution of *N*-succinimidyl 4-azido 2,3,5,6-tetrafluorobenzoate (0.488 g, 1.47 mmol) in chloroform was added dropwise to a solution of diphenylphosphinomethane (0.566 g, 1.47 mmol) cooled to 0 °C under dry nitrogen atmosphere. The solution turned yellow, and the mixture was stirred for 6 h before the solvent was removed in a vacuum to give a pale yellow crystalline material. Recrystallization was carried out by dissolving the crude material in hot acetonitrile and cooled at 0 °C to get analytically pure material **6** (87.1% yield). ^{31}P NMR ($CDCl_3$) δ 11.3 (dt, $^2J_{PP} = 54.1$ Hz, $^4J_{PF} = 5.6$ Hz), −30.5 (d, $^2J_{PP} = 54.6$ Hz). ^{1}H NMR ($CDCl_3$) δ 2.86 (s, 4H), 3.39 (dd, 2H, $^2J_{PH} = 12.2$ Hz), 7.1−7.9 (m, 20H). ^{19}F NMR ($CDCl_3$) δ −138.81 (m, 2F), −154.05 (m, 2F). Anal. Calcd for $C_{36}H_{26}N_2F_4P_2O_4$: C, 62.78; H, 3.81; N, 4.07. Found: C, 62.12; H, 3.87; N, 4.15.

A solution of 4-azido 2,3,5,6-tetrafluoromethylbenzoate (2.5 g, 10.03 mmol) in chloroform was added dropwise to a solution of diphenylphosphinomethane (3.86 g, 10.01 mmol) cooled to 0 °C under dry nitrogen atmosphere. The solution turned yellow, and the mixture was stirred for 6 h before the solvent was removed in a vacuum to obtain a pale yellow solid which was recrystallized by dissolving it in hot acetonitrile followed by slow cooling at room temperature to obtain **7** (82.4% yield). ^{31}P NMR ($CDCl_3$) δ 11.8 (dt, $^2J_{PP} = 53.5$ Hz, $^4J_{PF} = 6.6$ Hz). −30.5 (d, $^2J_{PP} = 53.6$ Hz). ^{1}H NMR ($CDCl_3$) δ 3.36 (dd, 2H, $^2J_{PH}$ =12.3 Hz), 3.87 (s, 3H), 7.1−7.9 (m, 20H). ^{19}F NMR ($CDCl_3$) δ −144.00 (m, 2F), −154.80 (m, 2F). Anal. Calcd for $C_{33}H_{25}NF_4P_2O_2$: C, 65.45, H, 4.13; N, 2.31. Found: C, 66.15; H, 4.15; N, 2.11.

A solution of 4-azido 2,3,5,6-tetrafluorobenzamide (2.32 g, 10.99 mmol) in toluene was slowly added to diphenylphosphinomethane (dppm, 4.22 g, 10.97 mmol) in tolune at 0 °C. The reaction mixture was stirred for 3 h and monitored by ^{31}P NMR spectroscopy. The solvent was removed in a vacuum to obtain a crystalline solid which was dissolved in hot acetonitrile and recrystallized in the presence of hexane to obtain a pure solid **8** (78.5% yield). ^{31}P NMR ($CDCl_3$) δ 11.3 (dt, $^2J_{PP} = 54.1$ Hz, $^4J_{PF} = 5.6$ Hz), −30.5 (d, $^2J_{PP} = 54.6$ Hz). ^{1}H NMR ($CDCl_3$) δ 6.61, 6.56 (s, 2H), 3.39 (dd, 2H, $^2J_{PH} = 12.2$ Hz), 7.1−7.9 (m, 20H). ^{19}F NMR ($CDCl_3$) δ −138.81 (m, 2F), −154.05 (m, 2F). Anal. Calcd for $C_{32}H_{24}N_2F_4P_2O$: C, 65.12; H, 4.06; N, 4.74. Found: C, 65.55, H, 4.15; N, 4.51.

Analytical Data for 9: (92.4% yield). ^{31}P NMR ($CDCl_3$) δ 11.6 (dt, $^2J_{PP} = 53.1$ Hz, $^4J_{PF} = 4.8$ Hz). −30.2 (d, $^2J_{PP} = 53.7$ Hz). ^{1}H NMR ($CDCl_3$) δ 3.28 (dd, 2H, $^2J_{PH} = 12.8$ Hz), 7.0−7.8 (m, 20H). ^{19}F NMR ($CDCl_3$) δ −56.8 (t, 3F, $^4J_{FF} = 21.6$ Hz), − 144.23 (m, 2F), −155.21 (m, 2F). Anal. Calcd for $C_{32}H_{22}NF_7P_2$: C, 62.43; H, 3.60; N, 2.28. Found: C, 62.01; H, 3.67; N, 2.15.

A solution of 4-azido 2,3,5,6-tetrafluorobenzamido lisinopril (25.95 mg, 0.032 mmol) in DMF was slowly added to diphenylphosphinomethane (12.4 mg, 0.032 mmol) in dry DMF at 0 °C. The reaction mixture was stirred for 3 h and monitored by ^{31}P NMR spectroscopy. The solvent was removed in a vacuum to obtain a pasty solid which was dissolved in CH_2Cl_2 and recrystallized to obtain solid **10**.

Analytical Data for 10: (76.5% yield). ^{31}P NMR ($CDCl_3$) δ 11.4 (dt, $^2J_{PP} = 45.3$ Hz, $^4J_{PF} = 6.1$ Hz), −29.2 (d, $^2J_{PP} = 45.8$ Hz). ^{1}H NMR ($CDCl_3$) δ 3.39 (dd, 2H, $^2J_{PH} = 12.1$ Hz), 7.1−7.9 (m, 20H). All other resonances coincide with native lisinopril. ^{19}F NMR ($CDCl_3$) δ −143.61 (m, 2F), −155.82 (m, 2F). Anal. Calcd for $C_{53}H_{52}N_4F_4P_2O_6$: C, 65.01; H, 5.36; N, 5.73 Found: C, 65.55, H, 5.23; N, 5.61.

Synthesis of Rh(III) Complexes 11−15. To $RhCl_3$ in chloroform (0.148 g, 0.71 mmol) were added a few drops of alcohol. The mixture was heated until it dissolved. The hot $RhCl_3$ solution was added slowly to a solution of **6** (0.487 g, 0.71 mmol) in chloroform, refluxed for 3 h, and monitored by ^{31}P NMR spectroscopy until the disappearance of phosphorus signals due to ligand **6**. The solvent was removed by a flash evaporator, and the orange-red solid was dissolved in a mixture of dichloromethane and hexane (8:2) and cooled at 0 °C to obtain a crystalline material **11** (78.5% yield). ^{31}P NMR ($CDCl_3$) δ 7.43 (dt,

(20) Pandurangi, R. S.; Lusiak, P.; Kuntz, R. R.; Volkert, W. A.; Rogowski, J.; Platz, M. S. *J. Org. Chem.* **1998**, in press.

(21) The following references are relevant to the NRCVAX system: (a) Gabe, E. G.; Page, Y. L.; Charland, J. L.; Lee, F. L.; White, P. S. *J. Appl. Crystallogr.* **22**, *384*, 1989. (b) Flack, L. *Acta Crystallogr. Sec. A* **39**, *876* 1983. (c) Johnson C. K.; ORTEP− A Fortran Thermal Ellipsoid Plot Program, Technical Report ORNL-5138, Oak Ridge, 1976. (d) Larson A. C. *Crystallographic Computing*; Munksgaard: Copenhagen, 1970; p 293. (e) Page, Y. L. J. *Appl. Crystallogr.* **1988**, *21*, 983. (f) Page, Y. L.; Gabe E. J. *J. Appl. Crystallogr.* **1979**, *12*, 464. (g) Rogers, D. *Acta Crystallogr. Sect. A* **1981**, *37*, 7.

$^2J_{PP}$ = 30.5 Hz, $^4J_{PF}$ = 5.3 Hz), 16.5 (m, $^1J_{P-Rh}$ =115.8 Hz, $^2J_{PP}$ = 24.2 Hz), 24.2 (m, $^1J_{P-Rh}$ =115.4 Hz, $^2J_{PP}$ = 24.6 Hz), 44.1 (dt, $^2J_{PP}$ = 15.2 Hz), ^{1}H NMR ($CDCl_3$) δ 2.81 (s, 4H), 4.18 (dd, 2H, $^2J_{PH}$ = 11.6 Hz), 5.20 (dd, 2H, $^2J_{PH}$ = 10.4 Hz), 6.6−7.6 (m, 40H). ^{19}F NMR ($CDCl_3$) δ −132.2 (m, 2F), −140.7 (m, 2F), −141.4 (m, 2F) −154.1 (m, 2F). ^{13}C NMR ($CDCl_3$) 28.4 (m, $^1J_{C-P}$ = 26.3 Hz) and 37.1 (m, $^1J_{C-P}$ = 28.3 Hz). Anal. Calcd for $C_{72}H_{52}N_4F_8P_4O_8$ $RhCl_3$: C, 54.54; H, 3.31; N, 3.54. Found: C, 55.11; H, 3.65; N, 3.61.

$RhCl_3$ (0.069 g, 0.329 mmol) was added to chloroform along with a few drops of alcohol and heated till it dissolved. The hot solution of $RhCl_3$ was added slowly to a solution of **7** (0.200 g, 0.329 mmol) in chloroform, refluxed for 3 h, and monitored by ^{31}P NMR spectroscopy until the disappearance of phosphorus signals due to ligand **7**. The solvent was removed by a flash evaporator to obtain an orange-red solid **12**. To get X-ray quality crystals, the solid was redissolved in hot $CHCl_3$ and slowly evaporated over a layer of hexane at room temperature (86.5% yield). ^{31}P NMR ($CDCl_3$) δ 6.15 (dt, $^2J_{PP}$ = 30.3 Hz, $^4J_{PF}$ = 5.3 Hz), 16.7 (m, $^1J_{P-Rh}$ =109.1 Hz, $^2J_{PP}$ = 27.1 Hz), 24.4 (m, $^1J_{P-Rh}$ =111.9 Hz, $^2J_{PP}$ = 23.5 Hz), 42.3 (dt, $^2J_{PP}$ = 15.8 Hz, $^4J_{PF}$ = 4.85 Hz). ^{1}H NMR ($CDCl_3$) δ 3.89 (s, 3H), 3.97 (s, 3H), 4.01 (m, 2H), 5.18 (dd, 2H, $^2J_{PH}$ = 12.3 Hz), 6.5−7.8 (m, 40H). ^{19}F NMR ($CDCl_3$) δ −132.9 (m, 2F), −140.9 (m, 2F), −143.8 (m, 2F) −153.9 (m, 2F). ^{13}C NMR ($CDCl_3$) 27.4 (m, $^1J_{C-P}$ = 24.8 Hz) and 36.1 (m, $^1J_{C-P}$ = 29.1 Hz). Anal. Calcd for $C_{68}H_{53}N_3F_8P_4O_4$ $RhCl_3$. CH_3CN: C, 55.93; H, 3.66; N, 2.88. Found: C, 55.32; H, 3.51; N, 2.81.

Analytical data for 13: (84.5% yield). ^{31}P NMR ($CDCl_3$) δ 6.83 (dt, $^2J_{PP}$ = 32.5 Hz, $^4J_{PF}$ = 5.6 Hz), 17.5 (m, $^1J_{P-Rh}$ =118.7 Hz, $^2J_{PP}$ = 23.8 Hz), 23.4 (m, $^1J_{P-Rh}$ =131.5 Hz, $^2J_{PP}$ = 27.1 Hz), 43.1 (dt, $^2J_{PP}$ = 14.2 Hz, $^4J_{PF}$ = 5.1 Hz). ^{1}H NMR ($CDCl_3$) δ 6.76, 6.56 (s, 2H), 4.12 (dd, 2H, $^2J_{PH}$ = 11.3 Hz), 5.28 (dd, 2H, $^2J_{PH}$ = 10.8 Hz), 6.6−7.6 (m, 40H). ^{19}F NMR ($CDCl_3$) δ −131.9 (m, 2F), −140.4 (m, 2F), −142.6 (m, 2F) −155.5 (m, 2F). ^{13}C NMR ($CDCl_3$) 28.9 (m, $^1J_{C-P}$ = 22.5 Hz) and 35.8 (m, $^1J_{C-P}$ = 29.1 Hz). Anal. Calcd for $C_{64}H_{48}N_4F_8P_4O_2$-$RhCl_3$: C, 55.33; H, 3.49; N, 4.04. Found: C, 55.28, H, 3.54; N, 4.09.

Analytical data for 14: (77.5% yield). ^{31}P NMR ($CDCl_3$) δ 6.89 (dt, $^2J_{PP}$ = 29.5 Hz, $^4J_{PF}$ = 5.7 Hz), 15.8 (m, $^1J_{P-Rh}$ =118.5 Hz, $^2J_{PP}$ = 23.9 Hz), 24.8 (m, $^1J_{P-Rh}$ =133.2 Hz, $^2J_{PP}$ = 28.6 Hz), 42.1 (dt, $^2J_{PP}$ = 16.2 Hz, $^4J_{PF}$ = 4.9 Hz). ^{1}H NMR ($CDCl_3$) δ 4.26 (dd, 2H, $^2J_{PH}$ = 11.3 Hz), 5.13 (dd, 2H, $^2J_{PH}$ = 11.8 Hz), 6.6−7.6 (m, 40H). ^{19}F NMR ($CDCl_3$) δ −56.5 (t, 3H, $^4J_{FF}$ = 18.3 Hz), −131.9 (m, 2F), −141.1 (m, 2F), −142.4 (m, 2F) −155.8 (m, 2F). ^{13}C NMR ($CDCl_3$) 26.4 (m, $^1J_{C-P}$ = 25.3 Hz) and 35.8 (m, $^1J_{C-P}$ = 28.0 Hz). Anal. Calcd for $C_{64}H_{44}N_2F_{14}P_4RhCl_3$: C, 53.41; H, 3.08; N, 1.95. Found: C, 53.35; H, 3.13; N, 1.88.

Analytical data for 15: (72.5% yield). ^{31}P NMR ($CDCl_3$) δ 6.53 (dt, $^2J_{PP}$ = 31.3 Hz, $^4J_{PF}$ = 4.8 Hz), 15.8 (m, $^1J_{P-Rh}$ =113.7 Hz, $^2J_{PP}$ = 24.8 Hz), 24.7 (m, $^1J_{P-Rh}$ =132.3 Hz, $^2J_{PP}$ = 26.6 Hz), 42.9 (dt, $^2J_{PP}$ = 15.8 Hz, $^4J_{PF}$ = 4.9 Hz). ^{1}H NMR ($CDCl_3$) δ 4.32 (m, 2H, $^2J_{PH}$ = 12.6 Hz), 5.10 (m, 2H, $^2J_{PH}$ = 11.6 Hz), 6.6−7.6 (m, 40H). All other resonances coincide with native lisinopril. ^{19}F NMR ($CDCl_3$) δ −133.4 (m, 2F), −141.2 (m, 2F), −142.4 (m, 2F) −155.8 (m, 2F). ^{13}C NMR ($CDCl_3$) 28.1 (m, $^1J_{C-P}$ = 23.7 Hz) and 37.9 (m, $^1J_{C-P}$ = 29.9 Hz). Anal. Calcd for $C_{106}H_{104}N_8F_8P_4O_{12}$: C, 58.77; H, 4.84; N, 5.18. Found: C, 58.68; H, 4.79; N, 5.24.

Synthesis of Pd(II) Complexes 16−20. A solution of $PdCl_2(PhCN)_2$ (0.139 g, 36 mmol) in dichloromethane (50 mL) was slowly added to a solution of **6** (0.250 g, 36 mmol) also in dichloromethane at 25 °C. After stirring for an hour, the solution was partially evaporated in a vacuum and treated with *n*-hexane to precipitate the Pd complex **16**. The solution was filtered, and the precipitate was washed (3 × 20 mL) with *n*-hexane and dissolved in hot acetonitrile. After slow evaporation of the solvent, orange-red crystalline material was obtained (78.6% yield). ^{31}P NMR (CD_2Cl_2) δ 25.7 (m, $^2J_{PP}$ = 27.8 Hz), −56.3 (b, $^2J_{PP}$ = 27.3 Hz). ^{1}H NMR ($CDCl_3$) δ 2.89 (s, 4H), 3.42 (dd, 2H, $^2J_{PH}$ = 13.2 Hz), 7.1−7.9 (m, 20H). ^{19}F NMR (CD_2Cl_2) δ −139.91 (m, 2F), −152.05 (m, 2F). Anal. Calcd for $C_{36}H_{26}N_2F_4P_2O_4PdCl_2$: C, 50.00; H, 3.03; N, 3.24. Found: C, 50.09; H, 3.07; N, 3.28.

Analytical Data for 17: (82.1% yield). ^{31}P NMR (CD_2Cl_2) δ 23.7 (m, $^2J_{PP}$ = 27.8 Hz), −58.3 (b, $^2J_{PP}$ = 27.3 Hz). ^{1}H NMR (CD_2Cl_2) δ 3.91 (s, 3H), 3.36 (dd, 2H, $^2J_{PH}$ = 13.8 Hz), 7.1−7.9 (m, 20H). ^{19}F NMR ($CDCl_3$) δ −141.10 (m, 2F), −152.80 (m, 2F). Anal. Calcd for $C_{33}H_{25}NF_4P_2O_2$ $PdCl_2$: C, 50.71; H, 3.23; N, 1.79. Found: C, 50.23; H, 3.29; N, 1.82.

Synthesis of 18. A solution of $PdCl_2(PhCN)_2$ (0.348 g, 90.7 mmol) in dichloromethane (50 mL) was slowly added to a solution of ligand **8** (0.520 g, 91.6 mmol) also in dichloromethane at 25 °C. After stirring for an hour, the solution was partially evaporated in a vacuum and treated with *n*-hexane to precipitate the Pd complex **18**. The solution was filtered, and the precipitate was washed (3 × 20 mL) with *n*-hexane and dissolved in hot acetonitrile. After slow evaporation of the solvent, orange-red crystals were obtained for further X-ray studies. (78.1% yield), (P═N) = 1245 cm^{-1}. ^{31}P NMR (CD_2Cl_2) δ 27.7 (m, $^2J_{PP}$ = 27.8 Hz), −53.2 (b, $^2J_{PP}$ = 27.7 Hz). ^{1}H NMR (CD_2Cl_2) δ 5.61, 6.22 (s, 2H), 7.1−8.0 (m, 20H), 3.38 (dd, 2H, $^2J_{PH}$ = 12.3 Hz), ^{19}F NMR (CD_2Cl_2) δ −141.2 (m, 2F), −153.15 (m, 2F). Anal. Calcd for $C_{32}H_{24}N_2F_4P_2PdCl_2 \cdot CH_3CN$: C, 50.56; H, 3.37; N, 5.21. Found: C, 50.38, H, 3.28; N, 5.36.

Analytical Data for 19: ^{31}P NMR (CD_2Cl_2) δ 26.7 (m, $^2J_{PP}$ = 25.8 Hz), −56.3 (b, $^2J_{PP}$ = 25.2 Hz). ^{1}H NMR (CD_2Cl_2) δ 3.56 (dd, 2H, $^2J_{PH}$ = 12.8 Hz), 7.1−7.9 (m, 20H). ^{19}F NMR (CD_2Cl_2) δ −55.9 (t, 3F $^4J_{FF}$ = 19.8 Hz), − 140.23 (m, 2F), −151.42 (m, 2F). Anal. Calcd for $C_{32}H_{22}NF_7P_2$ $PdCl_2$: C, 48.55; H, 2.81; N, 1.77. Found: C, 48.48; H, 2.79; N, 1.83.

Analytical Data for 20: ^{31}P NMR (CD_2Cl_2) δ 28.1.7 (m, $^2J_{PP}$ = 25.8 Hz), −54.3 (b, $^2J_{PP}$ = 27.2 Hz). ^{1}H NMR (CD_2Cl_2) δ 3.46 (dd, 2H, $^2J_{PH}$ = 11.8 Hz), 7.1−7.9 (m, 20H). ^{19}F NMR (CD_2Cl_2) δ −140.61 (m, 2F), −152.32 (m, 2F). Anal. Calcd for $C_{53}H_{52}N_4F_4P_2O_6PdCl_2$: C, 55.10; H, 4.54; N, 4.85. Found: C, 55.16, H, 4.60; N, 4.78.

Results and Discussion

I. Synthesis, Spectroscopy, and Coordination Chemistry of Rh (III) and Pd (II) Perfluoroaryl (iminophosphorano)-phosphines. Iminophosphoranes are known to display versatile bonding interactions in both coordination and organometallic chemistry.[17] The incorporation of an iminophosphorane moiety with the other donor atoms to form a bidentate chelating framework or selective oxidation of one of the arms of diphosphines leading to asymmetric (iminophosphorano)phosphine introduces mixed ligating centers P(III) and P(V) and has been a subject of extensive research in the last 7 years.[17−22] For example, reactions of functionalized perfluoroaryl azides ($R\text{-}C_6F_4N_3$, R = succinimide, COOMe, $CONH_2$, and CF_3) with diphenylphosphinomethane (dppm) give the corresponding monosubstituted (iminophosphorano)phosphine in high yields (> 90%, Scheme 1). Generally, these reactions are selective in oxidizing only one P(III) center in dppm. In fact, some of the functionalized aryl azides ($R = CONH_2$, CF_3, COOMe etc.) when used 2−3-fold excess over dppm produce mono-oxidized derivatives in >85% yield. Succinimido functionalized perfluoroaryl azides are useful precursors of BFCAs since they can be conjugated to a biomolecule or pharmacophore at one end and can be derivatized by a chelating framework at the other end. For example, succinimido perfluoroaryl azide **1** is conjugated to lisinopril at one end, and at the other end, N_3 is oxidized selectively by one of the phosphorus of dppm to yield **10** in good yields (>75%). All of the iminophosphoranes are characterized by multinuclear NMR (^{31}P, ^{1}H, ^{13}C, and ^{19}F), IR, and elemental analysis.

II. X-ray Structural Investigations. Single-crystal X-ray structural investigations on the Rh(III) complex **12** and Pd(II) complex **18** are determined to confirm the conclusions drawn

(22) (a) Miles, J. S.; Visscher, M. O.; Carlton, K. G. *Inorg. Chem.* **1974**, *13*, 1632. (b) Imhoff, P.; Elsevier: C. J.; Stam C. H. *Inorg. Chim. Acta* **1990**, *175*, 209. (c) Imhoff, P.; Asselt, R. V.; Elsevier: C. J.; Zoutberg, M. C.; Stam C. H. *Inorg. Chim. Acta* **1991**, *184*, 73. (d) Imhoff, P.; Elsevier, C. J. *J. Organomet. Chem.* **1989**, *369*, c61. (e) Imhoff, P.; Sylvia, C. A.; Elsevier, C. J. *Organometallics* **1991**, *10*, 1421.

Scheme 1

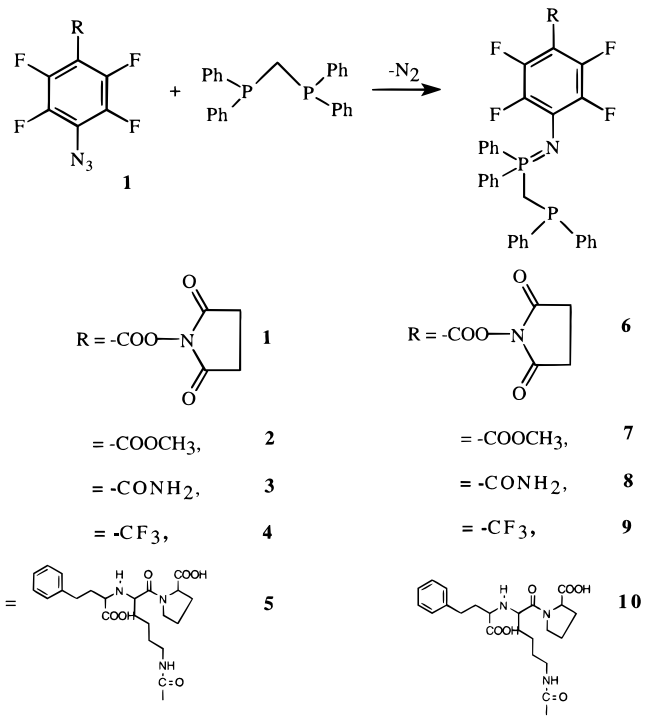

from the solution data (vide below) including the geometry and stereochemical features. ORTEP diagrams of the Rh(III) complex **12** and Pd(II) complex **18** with their atomic numbering schemes are shown in Figures 1 and 2 respectively. The structure of the Rh complex involves two ligands per metal center with one of the iminophosphoranes not involving in coordination to the metal and the other one forming a five membered ring with P(III) phosphorus. The availability of two different P(V) centers on the same molecule may be helpful in internal structural correlations and in addressing the hemilabile behavior of ligands, chelating effect, and stability factors.[24]

The Rh center has slightly distorted mer octahedral geometry with trans chloride ligands and two iminophosphorane units, one being away from the metal center such that the two P(III) phosphorus atoms are in cis arrangement. This observation from the crystal structure is also derived from the ^{31}P COSY NMR spectrum of **12** where P1 and P3 couple with a coupling constant of 30 Hz and is in the general range for cis coupled Rh complexes[24] (in fact, trans coupling is around 630 Hz, vide below). Compression of P(3)−Rh−N(2) [82.0° (4)] compared to P(3)−Rh−P(1) [98.8° (18)] indicates the ring strain which is the expected value for the related phosphorus−nitrogen systems.[25] A relative reduction of the angle P(4)−N(2)−C(59) [120.56° (13)] on the coordinated arm of the iminophosphorane is noted, compared to the bond angle P(2)−N(1)−C(26) [133.36° (8)] on the noncoordinated arm of the other iminophosphorane. The bond length for P═N involved in chelation [(1.606 Å(17)] is slightly elongated compared to free P═N [(1.578 Å (18)]. Similarly, the bond length N(2)−C(59) [1.411 Å (3)] on the coordinating part is also longer than the bond length N(1)−C(26) [1.352 Å(3)] on the noncoordinate part of iminophosphorane. In the uncomplexed iminophosphorane arm, the lone pair of electrons on nitrogen may delocalize through the perfluoroaryl group which may be responsible for the larger angle for P(2)−N(1)−C(26) [133.36° (8)] and shorter bond length for N(1)−C(26) [1.352 Å(3)], leaning toward linear geometry. However, the trigonal planar geometry around nitrogen center on the complex arm [P(4)−N(2)−C(59) [120.56° (13)] indicates the directional donation of the lone pair of sp^2 nitrogen to Rh metal. The similar lengthening of P═N bond lengths and reduction in bond angles is well-reported for Rh(I) complexes.[18,20] The Rh−Cl and Rh−P bond lengths in complex **12** can be discussed in relation to the trans influence of the chlorine and the iminophosphorane P═N group. For example, the P(3)−Rh bond [(2.305 Å (5)], being trans to chlorine is slightly longer compared to the P(1)−Rh bond [(2.289 Å (5)], reflecting the small, yet noticeable relative trans influence of the chlorine and P═N moiety, respectively. The Rh−Cl(2) bond trans to phosphorus [2.384 Å (5)] is longer than Rh−Cl trans to chloride (e.g., Rh−Cl3, 2.349 Å or Rh−Cl1, 2.365 Å) indicating that a larger trans influence for Rh−Cl(2) to phosphorus may be due to Rh−P π bonding. The elongation of Rh−Cl(2) compared to that of Rh−Cl(1) and Rh−Cl(3) is not unusual and in fact, reported for a number of dmpe complexes.[24f] The terminal chloride ligands Cl(1), Cl(2), and Cl(3) have meridional geometry common to many Rh(III) complexes with phosphorus−oxygen ligands.[26] Table 1 shows the summary of the crystallographic data on crystals **12** and **18**. Selected bond lengths and bond angles are given in Tables 2 and 3 for Rh and Pd complexes, respectively.

The ORTEP plot of **18** confirm the proposed five-membered metallacyclic structure with Pd(II) in square planar geometry. Pd metal is bound to the iminato nitrogen and P(III) center via cis disposition to form a five-membered chelate. The P−N bond length in **18** (1.60 Å) is in the normal range expected for P−N double bonds found in many reported complexes.[17] Similarly, the Pd−P bond length (2.224 Å) is also in the range normally expected for similar Rh and Pd complexes.

III. NMR Investigations. Rh(III) complexes are produced by the slow addition of a hot solution of $RhCl_3 \cdot xH_2O$ in $CHCl_3$ to the solution of ligands **6**−**10** in $CHCl_3$ in the presence of a few drops of ethyl alcohol, followed by refluxing it for 4 h (Scheme 2). Rh complex **12** is sparingly soluble in methanol and ethanol and is characterized by multinuclear NMR (^{31}P, ^{1}H, ^{19}F, and 2D COSY ^{31}P NMR), IR, and elemental analysis. ^{31}P NMR of **12** shows multiplets at δ 6.15, 16.7, 24.4, and 42.3 (Figure 3) with equal intensity (1:1:1:1). The multiplets at δ 16.7 and 24.4 appear to be similar with coupling constants 109.1 and 111.1 Hz, respectively. These coupling constants are typical of $^{1}J_{(P-Rh)}$ coupling reported for a number of Rh complexes.[23] On the basis of the coupling constant range, multiplets at δ 16.7 and 24.4 are assigned to P(III) phosphorus atoms. The two peaks also show characteristic large downfield shifts ($\Delta s = 47.2$ and 54.9, respectively) compared to that of ligand **7**, which is reminiscent of the shifts exhibited by P(III) coordination in several metal complexes.[22] The peak at δ 6.5 is a doublet and not shifted substantially compared to that of the P(V) phosphorus

(23) (a) Pregosin, P. S.; Kuntz, R. W. *^{31}P and ^{13}C NMR of Transition Metal Complexes*; Springer: Berlin, Heidelburg, New York, 1979. (b) Appleton, T. G.; Clark, H. C.; Manzer, L. E. *Coord. Chem. Rev.* **1973**, *10*, 335 (c) Goggin, P. L.; Knight J. R. *J. Chem. Soc. Dalton* **1972**, 704.

(24) (a) Garrou, P. E. *Chem. Rev.* **1981**, *81*, 829. (b) Chadwell, S. J.; Coles, S. J.; Edwards, P. G.; Hursthouse, M. B. *J. Chem. Soc. Dalton* **1995**, 3551. (c) Braunstein, P.; Matt, D.; Mathey, F.; Thaward, D. *J. Chem. Res.* (S) **1978**, 232. (d) Verkhade, J. G. *Coord. Chem. Rev.* **1972**, 9. (e) Garrou, P. E. *Inorg. Chem.* **1975**, *14*, 1435 (f) Suzuki, T.; Isobe, K.; Kashiwabara, K. *J. Chem. Soc. Dalton* **1995**, 3609.

(25) (a) Al-Soudani, A. R. H.; Batsanov, A. S.; Edwards, P. G.; Howard, J. A. K. *J. Chem. Soc. Dalton* **1994**, 987. (b) Knight, D. A.; Cole-Hamilton, D. J.; Cupertino, D. C.; Harman, M.; Hursthouse, M. B. *Polyhedron* **1992**, *11*, 1987. (c) Braunstein, P.; Matt, D.; Mathey, F.; Thaward, D. *J. Chem. Res.* (M) **1978**, 3041. (d) Skapski, A. C.; Stephans, F. A. *J. Chem. Soc. Dalton* **1973**, 1789.

(26) Braunstein, P.; Chauvin, Y.; Nahring, Y.; Decian, A. and Fischer, J. *J. Chem. Soc., Dalton* **1995**, 863.

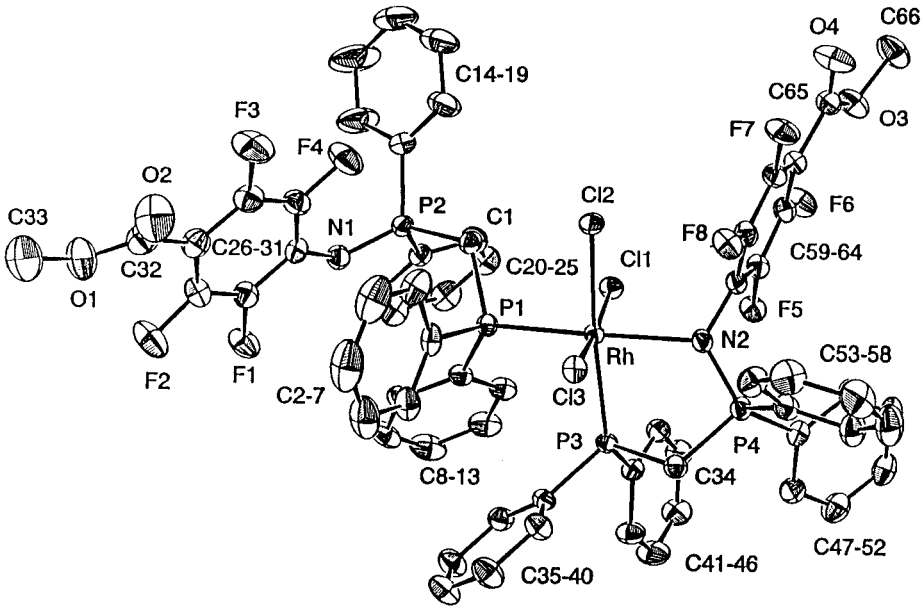

Figure 1. ORTEP diagram of Rh complex **12**.

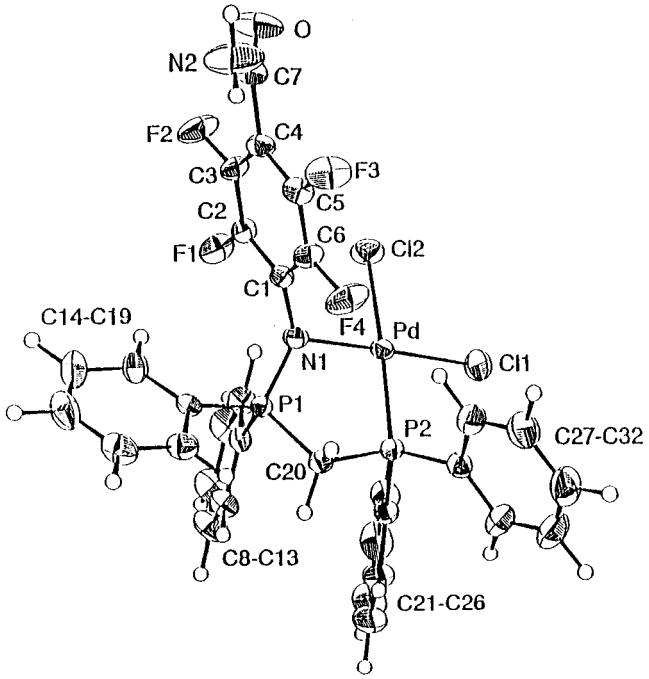

Figure 2. ORTEP diagram of Pd complex **18**.

Table 2. Bond Lengths and Bond Angles for Complex **12**

Rh1−Cl1	2.3658(5)	Cl1−Rh1−Cl2	84.755(18)
Rh1−Cl2	2.3840(5)	Cl1−Rh1−Cl3	172.004(17)
Rh1−Cl3	2.3496(5)	Cl1−Rh1−P1	86.958(17)
Rh1−P1	2.2894(5)	Cl1−Rh1−P3	104.17(17)
Rh1−P3	2.3054(5)	Cl1−Rh1−N2	88.65(4)
Rh1−N2	2.2316(16)	Cl2−Rh1−Cl3	87.249(18)
P2−N1	1.5786(18)	Cl2−Rh1−P1	88.709(17)
P4−N2	1.6064(17)	Cl2−Rh1−P3	168.529(18)
N1−C26	1.352(3)	Cl2−Rh1−N2	91.14(4)
N2−C59	1.411(3)	Cl3−Rh1−P1	92.765(17)
		Cl3−Rh1−P3	83.777(17)
		Cl3−Rh1−N2	91.63(4)
		P1−Rh1−P3	98.826(18)
		P1−Rh1−N2	175.59(4)
		P3−Rh1−N2	82.01(4)
		Rh1−P1−C1	108.66(7)
		Rh1−P1−C2	113.65(6)
		Rh1−P1−C8	115.84(7)
		N2−P4−C34	103.32(9)
		P2−N1−C26	133.36(15)
		Rh1−N2−P4	123.11(9)
		Rh1−N2−C59	116.32(12)
		P4−N2−C59	120.56(13)

in ligand **7** (δ 11.8) and, hence, indicates that it may not be involved in chelation to Rh via the nitrogen atom. On the other hand, the peak at δ 42.3 is shifted downfield ($\Delta s = 30.5$) with a value similar to the reported values for P(V) phosphorus in Rh(I) iminophosphorane complexes,[17] indicating that it may be involved in coordination to the metal center. Both peaks exhibit doublets with coupling constants 30.3 and 15.8 Hz ($^2J_{P-P}$), respectively. However, it is to be noted that the broad P(V) phosphorus signals are not well-resolved, masking additional information on long-range fluorine and Rh coupling. On the basis of the above observations, it can be safely assumed that two ligands are involved in Rh complex formation.

The inference of two ligands per metal center also comes from the investigations on ^{1}H, ^{19}F, and ^{13}C NMR of **12**. For example, ^{1}H NMR of **12** shows two distinct peaks (doublet of doublet, $^2J_{P-H} = 12.3$ Hz) at δ 4.01 and 5.18 (compared to the peak at δ 3.36, $^2J_{PH} = 12.3$ Hz in ligand **7**) assigned to two CH_2 groups of the two separate ligands, the latter peak being shifted further downfield which can be assigned to CH_2 of the P−C−P backbone in which both P(III) and P(V) are involved in coordination. ^{1}H NMR also shows two closely spaced peaks (3.89 and 3.91) assigned to two types of OCH_3 groups. Similarly, ^{19}F NMR shows four signals at δ −132.9, −140.9, −143.8, and −153.9 instead of the expected two signals of the AA′ XX′ pattern for the perfluoro core, as for example in ligand **7** (δ −144.0 and −154.0.8). On closer examination, it appears that two sets of fluorine signals (i.e., δ −143.8 and −153.9) are similar to the fluorine signals in ligand **7** and, hence, can be assigned to perfluoroiminophosphorane in which P═N is not coordinated to Rh. Further characterization of the Rh(III) complex is provided by ^{13}C NMR corroborating well with the inference of two ligands per metal center by showing two sets of multiplets (doublet of doublet) at δ 28.4 ($^1J_{C-P} = 26.4$ Hz) and 37.4 ($^1J_{C-P} = 32.6$ Hz), respectively for two different CH_2 groups on each of the P−C−P backbones of two ligands.

Although peaks due to P(V) phosphorus could be assigned, it is difficult to assign peaks at δ 16.7 and 24.4 as to which

Scheme 2

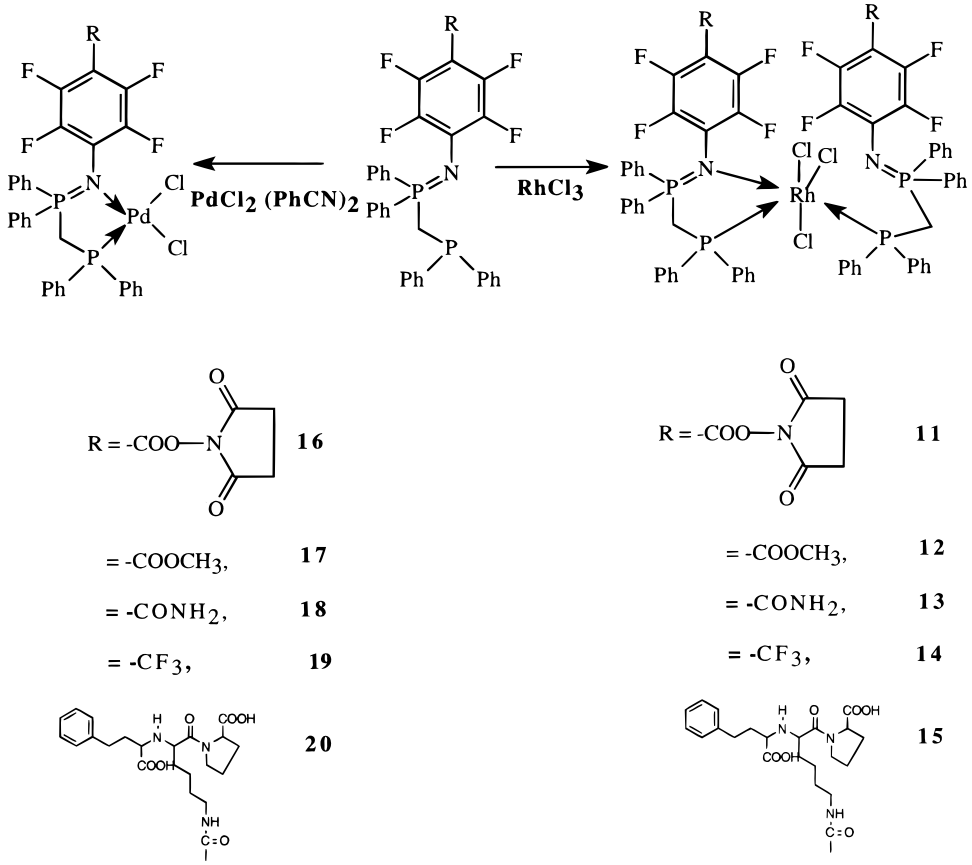

Table 3. Bond Lengths and Bond Angles for Complex **18**

Pd−C11	2.2927(10)	C11−Pd−C12	93.71(4)
Pd−C12	2.3577(9)	C11−Pd−P2	86.79(3)
Pd−P2	2.2248(9)	C11−Pd−N1	174.30(7)
Pd−N1	2.0798(24)	C12−Pd−P2	174.51(3)
P1−N1	1.6029(24)	C12−Pd−N1	90.57(7)
P1−C8	1.787(3)	P2−Pd−N1	89.32(7)
P1−C14	1.792(3)	N1−P1−C8	109.22(13)
P1−C20	1.795(3)	N1−P1−C14	115.68(12)
P2−C20	1.834(3)	N1−P1−C20	106.14(13)
P2−C21	1.808(3)	C8−P1−C14	108.66(13)
P2−C27	1.812(3)	C8−P1−C20	107.21(13)
N1−C1	1.399(3)	C14−P1−C20	109.60(13)
		Pd−P2−C20	105.81(9)
		Pd−P2−C21	115.14(11)
		Pd−P2−C27	117.06(10)
		C20−P2−C21	104.54(13)
		C20−P2−C27	102.67(13)
		C21−P2−C27	109.93(14)
		Pd−N1−P1	111.98(12)
		Pd−N1−C1	118.65(18)
		P1−N1−C1	127.23(19)
		N1−C1−C2	121.52(54)
		N1−C1−C6	122.86(24)

belongs to which phosphorus using 1D NMR spectrum alone. To understand the complicated coupling pattern and confirm the assignments to different phosphorus P(III) signals, a 2D ^{31}P COSY experiment was conducted. Figure 4 shows the 2D NMR spectrum for complex **12**. For simplicity, phosphorus peaks are numbered A, B, C, and D. To start with, A and D are already assigned to coordinated P(V) and noncoordinated P(V), respectively. Coupling of D with B, but not with C, indicates that D is connected to B on the same arm of iminophosphorane which is not coordinated to Rh. Hence, peak B can be assigned to P1(vide infra). Coupling of A with both C and B can be rationalized on the basis of ring formation through which A couples to B. The shape of both B and C peaks appear complicated owing to the coupling with phosphorus of the second ligand through the ring in addition to the existing coupling with P(V) of the same arm. The coupling constants around 23−28 Hz can be attributed to $^2J_{PP}$ coupling. The assignment of C to phosphorus P3 (Figure 1) involved in the ring formation with Rh is also based on the normal upfield shift due to effect often called "ring contribution" proposed by Garrou et al.[24] It has been shown that the phosphorus atom in a five-membered chelate ring gives a lower field resonance compared to a phosphorus atom not involved in the ring.[24b]

Functionalized Rh complexes (**11**, **13**−**15**) show similar NMR spectra including the one which is attached to lisinopril at the position para to perfluoroaryl azide group. On the basis of the similarity of the spectroscopic properties and X-ray structural investigations of **12** (vide infra), it is reasonable to assume that the lisinopril-conjugated Rh complex has also two ligands per metal center, which is also verified by conventional element analysis.

Unlike Rh complexes, Pd complexes of the functionalized perfluoroaryl derivatives have a relatively simple NMR pattern. For example, compound **18** shows downfield shifts of 56 ppm and 45 ppm for P(III) and P(V), respectively, after coordination. The magnitude of $^2J_{PP}$ coupling decreases to 25 Hz upon complexation. The complexation with Pd II with **8** is expected to withdraw electron density away from the N−P−C−P skeleton and presumably cause a decrease in the s character within the P−C−P framework. The chemical constitution of **18** was confirmed by the single-crystal X-ray investigations.

IV. IC_{50} Measurements Using ACE Amidolytic Assay. ACE from rabbit lung is incubated with lisinopril derivatives

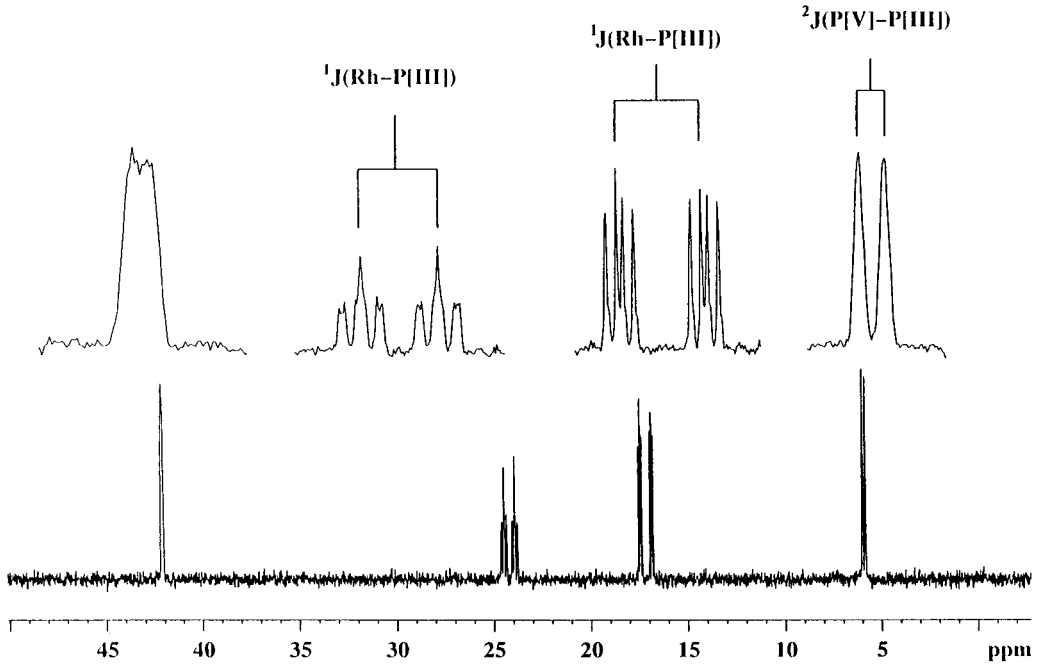

Figure 3. ^{31}P NMR spectrum of Rh complex.

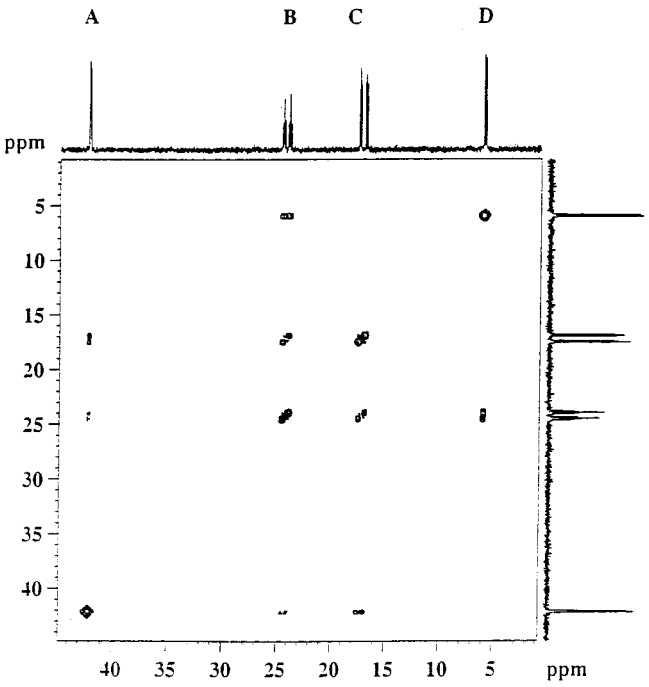

Figure 4. 2D ^{31}P COSY NMR spectrum of Rh complex **12**.

or metal conjugates at various concentrations in a mixture of methanol and buffer. The inhibition induced by modified lisinopril derivatives reduces the cleaving potency of ACE which results in the decreasing absorbance of the cleaved product of the substrate at 340 nm. The change in the percentage of inhibition is calculated by measuring the relative integration of peak areas. Lisinopril forms a positive control. Figure 5 shows the concentration dependence of lisinopril conjugates (**5**, **10**, **15**, and **20**) on their inhibitory potency compared to that of native lisinopril. IC_{50} values calculated from the graph for **12** and **18** indicates that functionalization at the primary amine site sustains the inhibitory potency at nM level, and hence, these derivatives should be useful for further radiochemical studies. IC_{50} values for the other derivatives are shown in Table 4.

In the absence of the availability of the crystal structure of ACE, studies on the determination of the binding sites of ACE revolve around the measurement of IC_{50} values for ACE inhibitors, functionalized by a variety of groups.[27,28] However, ACE is a metalloprotease enzyme similar to carboxypeptidase A[29] or thermolysin,[30] and the availability of the crystal structure of thermolysin and its binding studies with different substrates can be extended to understand the binding modes of ACE with ACE inhibitors. Of special interest was the bidentate coordination of the carboxylate oxygens next to the secondary amine group on lisinopril (**5** in Scheme 1). Along with the hydrophobic binding pockets with phenyl S^1, lysyl part $S_1{}^1$, and leucine $S_2{}^1$ these are found to be responsible for the tight binding of the ACE inhibitor to ACE. The importance of the carboxylic group of the *N*-carboxy alkyl fragment of ACE inhibitors is revealed by the marked decrease in inhibitor potency from 1.2 nM to 5.8 μM after replacing the carboxylic group with hydrogen (Table 9 in ref 8c). Our studies on the esterification of both carboxylic groups on lisinopril also resulted in the reduction of inhibitory potency from nM to μM levels.[14,15] The biological activity of ACE has long been known to be abolished by chelating agents such as EDTA, and in fact, the EDTA effect has led to the conclusion that ACE is a metalloenzyme.[32] The functional role of Zn in ACE-mediated hydrolysis of oligopeptides is shown to be similar to that of Zn in carboxypeptidase A[29] or thermolysin.[30,31] It is possible that ACE inhibitors may also bind to substrates other than ACE (e.g., in the deactivation of bradykinin[5]). However, the concordance of high-density

(27) Mendelsohn, F. A. O. *Clin. Exp. Pharmacol. Physiol.* **1984**, *11*, 431.
(28) Bernstein, K. E.; Martin, B. M.; Edwards, A. S.; Bernstein, E. A. *J. Biol. Chem.* **1989**, *264*, 11945.
(29) (a) Valle, B. L.; Glades, D. S.; Auld; Riordan J. F. In *Metal ions in Biology: Zinc Enzymes*; Spiro, T. G., Ed.; Wiley: New York, 1983; Vol. 5, pp 25−75. (b) Lipscomb, W. N.; Hartsuck, J. A.; Quiocho, F. A.; Reeke, G. N. *Proc. Natl. Acad. Sci. U.S.A.* **1969**, *64*, 28. (c) Vallee, B. L.; Rupley, J. A.; Coombs, T. L.; Neurath, H. *J. Biol. Chem.* **1960**, *235*, 64.
(30) (a) Holmquist, B. and Vallee, B. L. *J. Biol. Chem.* **1974**, *249*, 4601. (b) Kester, W. R.; Matthews, B. W. *Biochemistry* **1977**, *16*, 2506.
(31) Colman, P. M.; Jansonius J. N.; Matthews, B. W. J. *J. Mol. Biol.* **1972**, *70*, 701.
(32) Gonzalez, E. B.; Farkas, E.; Soudi, A. A.; Tan, T.; Yanovski, A. I.; Nolan, K. B. *J. Chem. Soc., Dalton Trans.* **1997**, 2377.

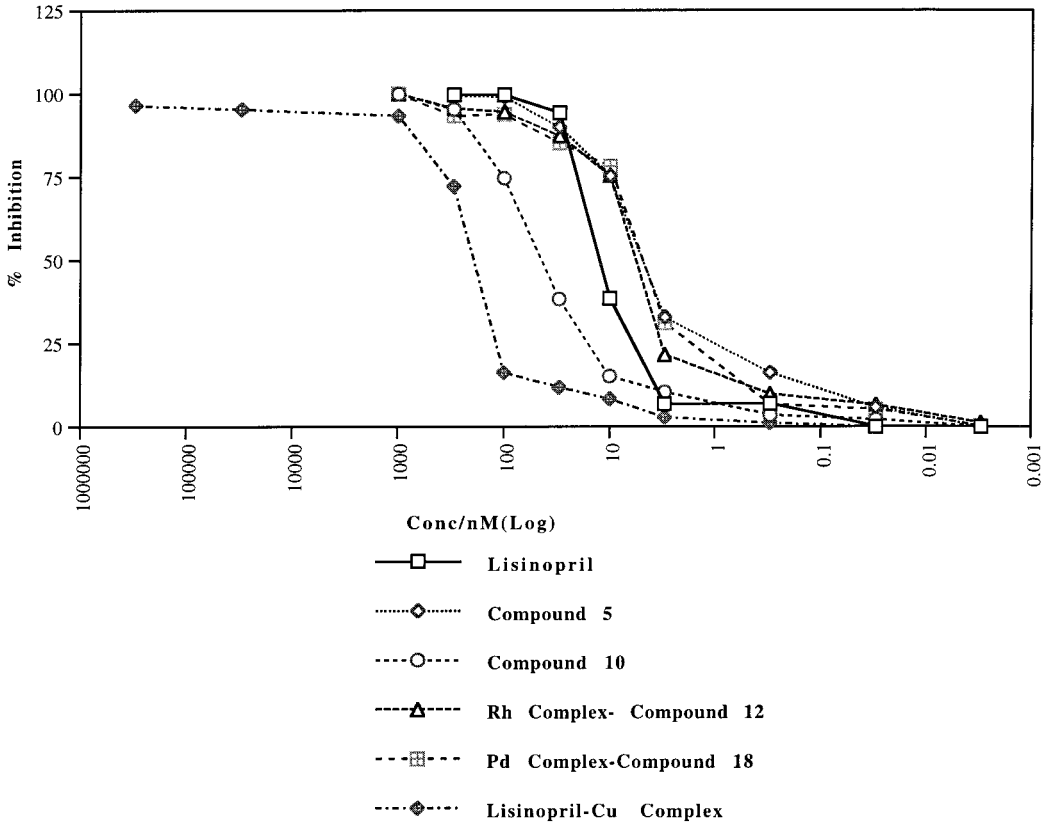

Figure 5. Concentration dependence of functionalized lisinopril derivatives **5**, **10**, **15**, and **20**.

Table 4. IC_{50} Values for Lisinopril Conjugates

compd	IC_{50} (nM)	ref
lisinopril	11.2	7c, d, 8c, 14, 15
I-125 351A	2.6	6c, 8c, 27
primary amine modified lisinopril **5**	0.62	14, 15
secondary amine modified lisinopril	30.2	14, 15
esterified lisinopril	201	14, 15
compound **10**	26	this work
Rh complex **12**	5.2	this work
Pd complex with **18**	8.9	this work
lisinopril−Cu complex[a]	267	this work

[a] Reference 32.

ACE binding with fibrotic tissues and the absence of carboxypeptidase or thermolysin at such sites makes ACE inhibitor scintigraphy feasible. Lisinopril conjugates bind ACE strongly (IC_{50} values are in nM range) which may be attributed to the availability of additional binding sites in the form of hydrophobic interactions and H-bonded interactions similar to *N*-carboxy alkyl dipeptides.[15] Recently, Gonzalez et al. have reported on a Cu(II) dimeric complex with lisinopril in which oxygen atoms of carboxylate and carbonyl groups as well as the secondary amine nitrogen of one of the lisinopril ligands occupy three positions in the basal plane of Cu, whereas the fourth position is occupied by the prolyl carboxylate of a second lisinopril ligand.[32] Our IC_{50} values, measured on a Cu−lisinopril conjugate, show a significant reduction in inhibitory potency to μM levels (Figure 5) indicating the sensitivity of substituents to the biological activity of lisinopril. In contrast, introduction of Rh and Pd on the long-chain end of the aliphatic primary amine function did not affect the inhibitory potency after functionalization. Such modified lisinopril derivatives may be amenable to noninvasive imaging of biological sites in vivo. However, the ultimate diagnostic applications demand high stability of the metal complex in vivo since demetalation would obscure the contrast between normal and fibrotic sites. The combination of two phosphines and one iminophosphorane may provide a much needed stability for a Rh(III) metal complex in biological conditions.

V. Conclusions

Functionalization of ACE inhibitors by Rh- and Pd-based BFCAs opens a possibilty of introducing clinically useful radionuclides to pharmacophores for in vivo tracking applications in humans. Measurement of IC_{50} values of lisinopril conjugates functionalized at various positions on lisinopril enable us to introduce relatively bulky chelating frameworks far away from the binding sites retaining the inhibitory potency in the postmodification stage. Selective oxidation of one arm of diphosphines by functionalized perfluoroaryl azides R-$C_6F_4N_3$ (R = COOMe, succinimide, CF_3, and lisinopril) lead to a combination of a phosphine−iminophosphorane framework suitable for introducing Rh(III) and Pd(II) precursors. Tailoring lisinopril through the primary amine functionalized perfluoroaryl azides with or without metal exhibited high inhibitory potency, retaining the character of native lisinopril. On the other hand, direct complexation with carboxylic oxygens of lisinopril by a metal abolishes the ACE activity, exemplified by the low IC_{50} value. Structural characterization of the Rh(III) complex perfluoroaryl (iminophosphorano)phosphine **12** by multiprobe NMR and single crystal X-ray crystallography revealed the presence of two ligands per metal center with two phosphines and only one of the iminophosphorane participating in coordination to Rh. These studies also confirmed that the electron-rich centers in BFCA−lisinopril conjugates are far away from the binding sites of lisinopril, verifying the retention of their inhibitory potency. These new findings on the retention of inhibitory potency of Rh and Pd functionalized lisinopril form the basis for introduction of ^{105}Rh and ^{109}Pd radiomarkers. The

synthesis and radiochemical characterization of ^{105}Rh and ^{109}Pd functionalized lisinopril derivatives and their biodistribution studies in animals are in progress and will be published elsewhere.

Acknowledgment. The work was supported by funds provided by DOE Grant DEFG0289ER 60875. NMR data were collected on instruments purchased with funds from NSF Grants 8908304 and 9221835. We appreciate the help of Dr. Guo and Mr. Gao of the NMR facility for help with the decoupling experiments. We are grateful to Professors Wynn Volkert and Robert Kuntz for helpful discussions and support. R.S.P. acknowledges the useful discussions with Professor Karl T. Weber of Internal Medicine.

Supporting Information Available: Crystal structure data on **12** and **18**, atomic coordinates and equivalent isotropic displacement parameters, selected interatomic distances, torsional angles, displacement parameters for hydrogen atoms, and intensity data (49 pages, print/PDF). See any current masthead page for ordering information and Web access instructions.

JA9802403